Supporting Information

Spörl et al. 10.1073/pnas.1118641109

SI Materials and Methods

Additional in Vivo Studies. The study for obtaining punch biopsies was approved by the Ethics Commission of Charité Berlin (EA4/019/11). Tissue samples were collected according to the recommendations of the current version of the Declaration of Helsinki as applicable to a nondrug study, as well as according to applicable laws for a nondrug study. All donors provided written, informed consent. The study was performed at St. Hedwig Hospital (Berlin, Germany). Six healthy volunteers (two male and four female; 22–30 y) participated in the study. MCTQ data were obtained as described in the main text. Analysis of cortisol and melatonin levels in saliva samples obtained throughout the day were performed by IBL International. Three-millimeter punch biopsies were obtained from the upper posterior area at seven time points throughout 1 d (0800 hours, 1200 hours, 1600 hours, 2000 hours, and 2400 hours and 0400 hours and 0800 hours the following day). Skin punches were subsequently incubated in PBS at 55 °C for 3 min to separate epidermis and dermis. Tissue samples were then snap frozen in liquid nitrogen and stored at −80 °C. RNA extraction and quality control from punch-biopsy epidermis was performed by Miltenyi Biotec using the TRIzol method. Out of 42 samples, 3 (two 0800-hour samples of the first day and one 0800-hour sample of the second day) did not show sufficient RNA quality and were not processed further.

For the second suction-blister study, six volunteers of the previous study (see *Material and Methods* in the main text) were recruited. Epidermal tissue samples were collected according to the recommendations of the current version of the Declaration of Helsinki as applicable to a nondrug study, as well as according to applicable laws for a nondrug study. All donors provided written, informed consent. Suction-blister samples were obtained at the study center of Beiersdorf AG and approved by the Beiersdorf AG Legal Review Board. Collecting and processing of suction-blister samples and saliva samples were performed similar to the previous study. Saliva samples were obtained at 0700 hours and 1900 hours for two consecutive days. Suction blisters were harvested at 0930 hours and 2130 hours for two consecutive days. Suction-blister samples obtained at the second day were exposed to UV radiation (solar-simulated radiation, 1.25 minimal erythemal dose) because of a study setup for a different investigation. We found no significant variation in amplitudes of oscillating genes between UV-exposed and non-UV-exposed days.

Microarray Analysis, Data Evaluation, and Bioinformatics Methods. RNA extraction and quality control from suction-blister epidermis was performed by Miltenyi Biotec using the TRIzol method. We obtained RNA with sufficient quality for further processing from 19 out of 20 subjects. Linear amplification and labeling of RNA and hybridization of Agilent Whole Genome Oligo Microarrays 4x44k (Agilent Technologies) using 1.2–1.65 μg of Cy3-labeled cRNA was performed by Miltenyi Biotec, essentially as reported in ref. 1. Raw data of the hybridized microarrays were normalized using the Bioconductor R-Project package Linear Models for Microarray Data ("limma") (2). Background correction was performed using the "normexp" function and the between-array-normalization "quantile" (3). An offset of 20 was added to stabilize the background correction, and, subsequently, signals were log2 transformed. Genes were considered to be expressed if the background subtracted signal was above 2.6 times the SD of the background signal in at least 75% of the microarrays. For statistical analysis, each microarray was assigned to its corresponding time-group (i.e., 0930 hours, 1430 hours, or 1930 hours). Subsequently, a moderated F-Test of the empirical Bayes statistics for differential expression ("ebayes" function of the limma package) was applied to test differential gene expression between the respective groups for statistical significance (4). False-discovery rate was accounted for by calculating the q value (5), and a q value of <5% was considered statistically significant. Genes showing significant diurnal expression patterns were tested for overrepresentation in Kyoto Encyclopedia of Genes and Genomes pathways by applying the "hyperGTest" function, which is included in the "GOstats" package. Principle component analysis was performed by the "prcomp" function, which is part of the "stats" package in R-Project.

Microarray analysis of NHEKs carrying KLF9 or GFP expression constructs (see *SI Materials and Methods, Vector Generation, Lentivirus Production, Precipitation, and Transduction* below for details) were performed similarly. We determined differentially expressed genes using an ANOVA test with a false-discovery rate of 0.1 and a minimal mean fold change of 2.

All microarray raw data were deposited in the GEO database and can be accessed under accession no. GSE36014. Suction-blister data have been deposited in the GEO database under accession no. GSE35635.

Overlap of KLF9 targets with circadian genes from suction blisters. Genes commonly indicated as expressed in both microarray sets were selected. The false-discovery rate for the selection of daytime-dependent genes was adjusted to 0.1, and the overlap with the KLF9 targets was determined using the annotated gene symbols. The number of down- and up-regulated KLF9 targets was tested for overrepresentation within the circadian genes using Fisher's test considering a P value below 0.05 as significant.

Promoter analysis. Genomic sequences from −1,000 to +1,000 relative to the potential transcription start site were extracted for all protein coding genes annotated in the Ensembl database. As described earlier, KLF9 binds to SP1-like motifs in the promoter region of its target genes (6, 7). Because there are no individual matrices for binding motifs of KLF9 neither in the Transfac nor in the Jaspar database, three matrices related to SP1-binding motifs from the Transfac public version (V7.0) (8) were used for the analysis. Binding affinities in terms of Transcription Factor Affinity Prediction (TRAP) scores were calculated according to the published algorithm (9) for all promoters. A background set of noncircadian, non-KLF9 target genes was defined by the following parameters: false discovery rate (fdr) for suction-blister and for KLF9-overexpression data, >0.5; mean ratio in KLF9 overexpression data, <1.4 (3,019 genes in total). To match the size of the foreground sets (putative circadian KLF9 targets), a number of nonoverlapping sets of equal size was randomly sampled out of the whole background set (64 sets for down-regulated and 137 sets for the up-regulated circadian KLF9 targets, respectively). Statistical significance for a difference between TRAP scores of the foreground sets and all paired background sets was determined using the Mann–Whitney U test. Resulting P values were plotted in a density plot. For defining the significance of a specific Transfac motif for a particular test set the geometric means of all corresponding, P values were used.

Simulation of three-time-point sampling. To test whether a three-time-point sampling strategy is feasible to identify circadian regulated genes with reasonable sensitivity and specificity, we used a simulation approach with semisynthetic time series. We first defined robustly circadian genes from the liver transcriptome dataset published by Hughes et al. (10) and mixed them with truly noncircadian genes. To this end, probe-set time series were fitted to a cosine model and resulting P values were fdr-adjusted for mul-

tiple testing. Probe sets with a q value ≤ 0.05 and amplitude of ≥ 0.5 were considered as robustly circadian. A background set was generated by using probe sets with q values of >0.5 and amplitude of <0.05. Subsequently, the top 100 circadian or all circadian probe sets, respectively, were combined with the background probe sets (n = 5,061) and used as test set for the simulation. Secondly, we took systematic 3-time-point samples (5-h intervals spanning the whole circadian cycle) from these time series and transformed each value (as mean) into normally distributed 10 or 20 values with SDs similar to those of our epidermal transcripts, thereby simulating 3-time-point expression profiles of 10 or 20 subjects with realistic intersubject variability. To estimate such variability, SDs for all time points and all probe sets were calculated for the suction-blister data and plotted in a histogram. An intermediate SD of 0.25, as well as a substantially lower (0.0625) and higher (1) SD, was used for the simulation. The resulting semisynthetic dataset was subjected to empirical Bayes test statistic as used in the suction-blister study. The P values were fdr-adjusted, and all q values were sorted, starting with the lowest. To validate the performance of the test, true-positive and false-positive rates were calculated for the stepwise increasing sets starting with the lowest q value until the last value. The whole procedure was performed 38 times, with datasets shifting 1 h in the start time in each run. Mean values of all simulations were calculated and plotted in receiver operating characteristic (ROC) curves. The area under the curve (AUC) was determined as a numerical measurement of the quality of the test and is depicted in Table S2.

Cell Culture, Bioluminescence Recording, and Data Evaluation. Normal human epidermal NHEKs of three donors (NHEK pool) were purchased from Lonza, seeded in 75-cm^2 plastic flasks and cultured in complete Keratinocyte Growth Medium 2 (KGM-2) with growth factor supplements (Lonza) and 1 mM $CaCl_2$. When indicated cells were cultivated in KGM-2 lacking growth factors (autocrine conditions). Cells were cultivated at 37 °C, 7% (vol/vol) CO_2 and 95% (vol/vol) relative humidity. Cells were trypsinized and subcultured by standard methods when approaching ∼80% confluence or grown into postconfluence for in vitro differentiation studies (11). For *Klf9* expression analysis in epidermal stem cells, transit amplifying cells and fully differentiated epidermis validated cell fractions from (12) were used.

For live-cell bioluminescence monitoring, NHEK reporter cells were grown to confluence in 35-mm dishes and subsequently switched to autocrine growth conditions. At 1 d postconfluence, cells were synchronized with 50% (vol/vol) FCS (PAA) for 1 h. Following synchronization, medium was changed to autocrine KGM-2 containing 25 mM Hepes and 250 μM D-luciferin (Biotherma). Temperature profiles (12 h 37 °C/12 h 33 °C temperature cycle with 2-h transitions) were applied using a KBF115 incubator (Binder), and bioluminescence recordings were performed using a LumiCycle (Actimetrics). After bioluminescence recording over 5–8 d, data were analyzed using ChronoStar software (13). Raw data were detrended by dividing data points by the 24 h running average. For details, see ref. 13. Bioluminescence measurements in U2OS reporter cells were performed as described previously (13).

For temperature compensation experiments, HaCaT keratinocytes carrying a *Bmal1:luc* promoter reporter (14) were grown in DMEM, 10% (vol/vol) FCS, 1% penicillin/streptomycin and 25 mM Hepes at 37 °C and 5% (vol/vol) CO_2. For bioluminescent recording, 200,000 cells were seeded in 35-mm dishes. Following synchronization with 1 μM dex (Sigma-Aldrich) for 30 min, medium was changed to phenol-red free DMEM (PAA) containing 10% (vol/vol) FCS, 1% penicillin/streptomycin, 25 mM Hepes, and 250 μM D-luciferin (Biotherma). Subsequently, individual cultures were cultivated at different temperatures (33–39 °C). Bioluminescence recordings were performed using light-tight boxes with single photomultiplier tubes (Hamamatsu Photonics). Different temperatures were applied using a heating plate at the bottom of individual boxes controlled by a Jumo Imago 500 control unit. This setup was custom-built by the Technische Werkstätten Charité (Berlin, Germany). After bioluminescence recording over 7 d, data were detrended as described previously (13). The Q_{10} values were calculated as follows:

$$Q_{10} = \left(\frac{R2}{R1}\right)^{\frac{10}{T2-T1}},$$

where R is the rate of cycles per day, and T is the temperature.

Cotransactivation Assay. To test transactivation from E-boxes within the *Klf9* gene by CLOCK/BMAL1, 100,000 HEK293 cells were seeded into 24-well plates grown in DMEM (PAA), 10% (vol/vol) FCS (PAA), 1% penicillin/streptomycin (PAA), and 25 mM Hepes (Roth). Twenty-four hours later, cells were transfected using Lipofectamine 2000 reagent (Invitrogen) as previously described (15), with the following constructs: 50 ng of pSG-*Klf9:luc* construct (promoter clone ID S109468; Switch Gear Genomics) was cotransfected with 300 ng each of pDest26-Clock and pDest26-Bmal1, as well as with 150 ng of pDest26-Cry1 when indicated. In addition, as a transfection control, 50 ng of phRL-SV40 renilla luciferase plasmid was cotransfected. Each transfection reaction was supplemented with pDest26-βGal to reach 1,200 ng DNA in total. Forty-eight hours after transfection, cells were harvested, and luciferase activity was measured using the Dual-Luciferase Reporter Assay System (Promega) and the Orion Microplate Luminometer (Berthold). Results are averages of four independent cotransfection assays, each performed in triplicates, and are shown as fold induction to *Klf9:luc* basal activity.

Vector Generation, Lentivirus Production, Precipitation, and Transduction. A lentiviral expression vector for *Klf9* C-terminally fused to the V5 epitope was generated using the Gateway technology (Invitrogen). A gateway entry clone (pENTR221) comprising the full ORF of the *Klf9* gene was purchased from Thermo Fisher Scientific. The *Klf9* ORF was transferred into the lentiviral expression vector pLenti6/V5-DEST Gateway Vector using Gateway LR Clonase enzyme mix (Invitrogen) according to instructions of the manufacturer.

Lentiviruses containing a 0.9-kb fragment of the *Bmal1* promoter driving luciferase (16), shRNAmir knockdown constructs targeting *Klf9* and a nonsilencing control (Thermo Scientific) or pLenti6 expression constructs for Klf9_V5 and GFP, respectively, were generated as described (16). Lentiviral supernatant was concentrated by precipitation for 3–5 h using 8% (vol/vol) polyethylene glycol 6000 (PEG600; Sigma-Aldrich) in 1.6 M NaCl at 4 °C. Lentiviral particles were harvested at 4,000 × g, 4 °C for 30 min and resuspended in cold 1× PBS. NHEK cells were grown in 6-well or 96-well dishes to 30–50% confluence and infected using a final volume of 1/20–1/40 of 100× concentrated lentivirus and 8 μg/mL protamine sulfate (Sigma-Aldrich). Depending on the downstream application cells were selected for 24 h after transduction using 10 μg/mL puromycin or left untreated (proliferation assays).

Real-Time qPCR. Cells were harvested by trypsin incubation for 5 min at 37 °C and stored at -80 °C. Total RNA was isolated using the High Pure RNA Isolation Kit (Roche Diagnostics) according to the instructions of the manufacturer. Following RT-PCR (High Capacity cDNA Reverse Transcription Kit; Applied Biosystems), cDNA was loaded on a custom made TaqMan Custom Array containing primer pairs for 48 genes, which was obtained from Applied Biosystems. Quantitative real-time PCR was performed using the 7900HT Fast Real-Time-PCR System (Applied Biosystems). Expression data were normalized to ribosomal 18S RNA or several housekeeping genes [18S, Gapdh, Krt10, Krt14, and TATA box binding protein (Tbp)], and relative quantification (RQ) of gene expression was assessed by comparative ΔCT

analysis. For in vitro time-series analysis, datasets from each individual gene were detrended applying a linear fit and statistical analysis for circadian gene expression was performed using CircWave software (17).

For analysis of knockdown efficiency, U2OS were harvested 5 d after transduction with shRNA constructs for qPCR analysis (see ref. 13 for details). *Klf9* mRNA levels were analyzed using a QuantiTect Primer Assay (QT00208537; Fermentas) and normalized to *Gapdh*.

Immunofluorescence and Western Blot Analysis. For immunostaining, cells or human paraffin-embedded skin sections were fixed in acetone/methanol 1:1 for 30 min at −20 °C and washed with PBS. Cells were blocked with 1% BSA for 30 min and then incubated with primary antibodies (10 μg/mL) in 1% BSA for 1 h. Antibodies detecting the V5 epitope and KLF9 were purchased from Abcam and Sigma-Aldrich, respectively. After incubation cells were washed with PBS. Samples were then incubated for 1 h with 0.1% BSA solution containing fluorescent-labeled secondary antibody (AlexaFluor 488 goat anti-rabbit IgG; Molecular Probes). After extensive washing with PBS, samples were stained with DAPI (4′-6-diamidino-2′-phenylindol-dihydrochloride), and fluorescent images were obtained using a digital fluorescence microscope (BZ-8000; Keyence) or a Leica TSC SP5 confocal microscope (Leica Microsystems). Western blot analysis was performed using standard protocols, and KLF9_V5 fusion protein was detected using a monoclonal rabbit antibody against the V5 epitope (Abcam).

Proliferation Assays. For real-time measurements of cell proliferation, an impedance-based real-time cell analyzing system (xCELLigence; Roche Diagnostics) was used. Cells were cultivated in 96-well culture plates (E-plates) containing microelectrodes at the bottom of each well. Validity of this system for assessing proliferation in primary keratinocytes has been shown previously (18). A total of 2,500 keratinocytes/well were seeded into E-plates and cultivated for 48 h. Subsequently, cells were infected with lentivirus as described above. Lentiviral titers were adjusted to ensure transduction efficiency of ≥80%, and cells were cultivated without selection agent to exclude side effects on proliferation. Cell growth was subsequently monitored in 2 h intervals for 4–6 d. The impedance signal (cell index) was normalized to the time of virus application (i.e., all curves were set to a cell index value of 1). Real-time measurements were validated using endpoint-based cell-count assays. Cells were either counted by flow cytometry (CasyCount; Roche Diagnostics) or by automated microscopic cell count of DAPI-stained nuclei (Scan ^ R; Olympus).

Chromatin Immunoprecipitation (ChIP). U2OS cells were grown in 15-cm dishes to 95% confluence. Cells were synchronized with 1 μM dexamethasone for 1 h and harvested after 20 and 32 h. Cross-linking, chromatin preparation, and chromatin immunoprecipitation was performed as described in ref. 19 with modifications. Cells were sonicated on ice for 15 s five times with 50% setting followed by centrifugation for 10 min (13 krpm). Supernatants were diluted in buffer (1.1% Triton X-100, 2 mM EDTA, 150 mM NaCl, 20 mM Tris-HCl, pH 8.1) and incubated with anti-BMAL1 antibody (20), a gift from Michael Brunner (University of Heidelberg, Heidelberg, Germany), for 1 h rotating (RT), before adding of agarose-A bead slurry in the same buffer and 1 h rotating (RT). Precipitates were washed sequentially in TSE I (0.1% SDS, 1% Triton X-100, 2 mM EDTA, 20 mM Tris-HCl, pH 8.1, 150 mM NaCl), TSE II (0.1% SDS, 1% Triton X-100, 2 mM EDTA, 20 mM Tris-HCl, pH 8.1, 500 mM NaCl), TSE III (0.25 M LiCl, 1% NP-40, 1% deoxycholate, 1 mM EDTA, 10 mM Tris-HCl, pH 8.1), and TSE IV (10 mM Tris-HCl, pH 8.1, 150 mM NaCl, 1 mM EDTA). Cross-linking was reversed at 65 °C in (20 mM Tris-HCl, pH 7.5, 150 mM NaCl, 2 mM EDTA, 1% SDS) overnight. DNA fragments were purified with a QIAquick column Spin Kit (Qiagen) and eluted in 60 μl TE buffer. Q-PCR was performed with SYBR-green (Fermentas) on a CFX384 Real-Time PCR Detection System (Bio-Rad). Primers for three E-boxes and one control region without an E-box in the *Klf9* promoter and *Rev-erba* promoter were designed as follows: Klf9 E-box1: forward 5′-GTGCAGGGGCTAATTTCAAG-3′, reverse 5′-GCAGTTGAACAAACTGCCCTA-3′; Klf9 E-box2: forward 5′-CCCTGAAAGGGAGAGGTCTG-3′, reverse 5′-AGAACTGCCAGCCTCCAG-3′; Klf9 E-box3: forward 5′-AGGGCGTGCACCTCTCTT-3′, reverse 5′-CGGCTCCCTTGGAAAGAT-3′; Klf9 non E-box: forward 5′-TCGCGTTTACAAGTGTCGAG-3′, reverse 5′-AACGCTACAGTCCCAGCAAC-3′; Rev-erba: forward 5′-CTTCTCTCTCTCCCGGTCAC-3′, reverse 5′-CTGCAAACCTTGCAAACG-3′.

1. Duggan DJ, Bittner M, Chen Y, Meltzer P, Trent JM (1999) Expression profiling using cDNA microarrays. *Nat Genet* 21(1 Suppl):10–14.
2. Smyth GK, Speed T (2003) Normalization of cDNA microarray data. *Methods* 31: 265–273.
3. Ritchie ME, et al. (2007) A comparison of background correction methods for two-colour microarrays. *Bioinformatics* 23:2700–2707.
4. Smyth GK (2004) Linear models and empirical bayes methods for assessing differential expression in microarray experiments. *Stat Appl Genet Mol Biol*, 10.2202/1544-6115.1027.
5. Storey JD, Tibshirani R (2003) Statistical significance for genomewide studies. *Proc Natl Acad Sci USA* 100:9440–9445.
6. Sogawa K, Kikuchi Y, Imataka H, Fujii-Kuriyama Y (1993) Comparison of DNA-binding properties between BTEB and Sp1. *J Biochem* 114:605–609.
7. Kobayashi A, Sogawa K, Imataka H, Fujii-Kuriyama Y (1995) Analysis of functional domains of a GC box-binding protein, BTEB. *J Biochem* 117:91–95.
8. Matys V, et al. (2006) TRANSFAC and its module TRANSCompel: Transcriptional gene regulation in eukaryotes. *Nucleic Acids Res* 34(Database issue):D108–D110.
9. Roider HG, Kanhere A, Manke T, Vingron M (2007) Predicting transcription factor affinities to DNA from a biophysical model. *Bioinformatics* 23:134–141.
10. Hughes ME, et al. (2009) Harmonics of circadian gene transcription in mammals. *PLoS Genet* 5:e1000442.
11. Minner F, Herphelin F, Poumay Y (2010) Study of epidermal differentiation in human keratinocytes cultured in autocrine conditions. *Methods Mol Biol* 585:71–82.
12. Hildebrand J, et al. (2011) A comprehensive analysis of microRNA expression during human keratinocyte differentiation in vitro and in vivo. *J Invest Dermatol* 131:20–29.
13. Maier B, et al. (2009) A large-scale functional RNAi screen reveals a role for CK2 in the mammalian circadian clock. *Genes Dev* 23:708–718.
14. Spörl F, et al. (2011) A circadian clock in HaCaT keratinocytes. *J Invest Dermatol* 131: 338–348.
15. Bozek K, et al. (2009) Regulation of clock-controlled genes in mammals. *PLoS ONE* 4: e4882.
16. Brown SA, et al. (2005) The period length of fibroblast circadian gene expression varies widely among human individuals. *PLoS Biol* 3:e338.
17. Oster H, Damerow S, Hut RA, Eichele G (2006) Transcriptional profiling in the adrenal gland reveals circadian regulation of hormone biosynthesis genes and nucleosome assembly genes. *J Biol Rhythms* 21:350–361.
18. Spörl F, et al. (2009) Real-time monitoring of membrane cholesterol reveals new insights into epidermal differentiation. *J Invest Dermatol* 130:1268–1278.
19. Shang Y, Hu X, DiRenzo J, Lazar MA, Brown M (2000) Cofactor dynamics and sufficiency in estrogen receptor–regulated transcription. *Cell* 103:843–852.
20. Rey G (2011) Genome-wide and phase-specific DNA-binding rhythms of BMAL1 control circadian output functions in mouse liver. *PLoS Biol* 9:e1000595.

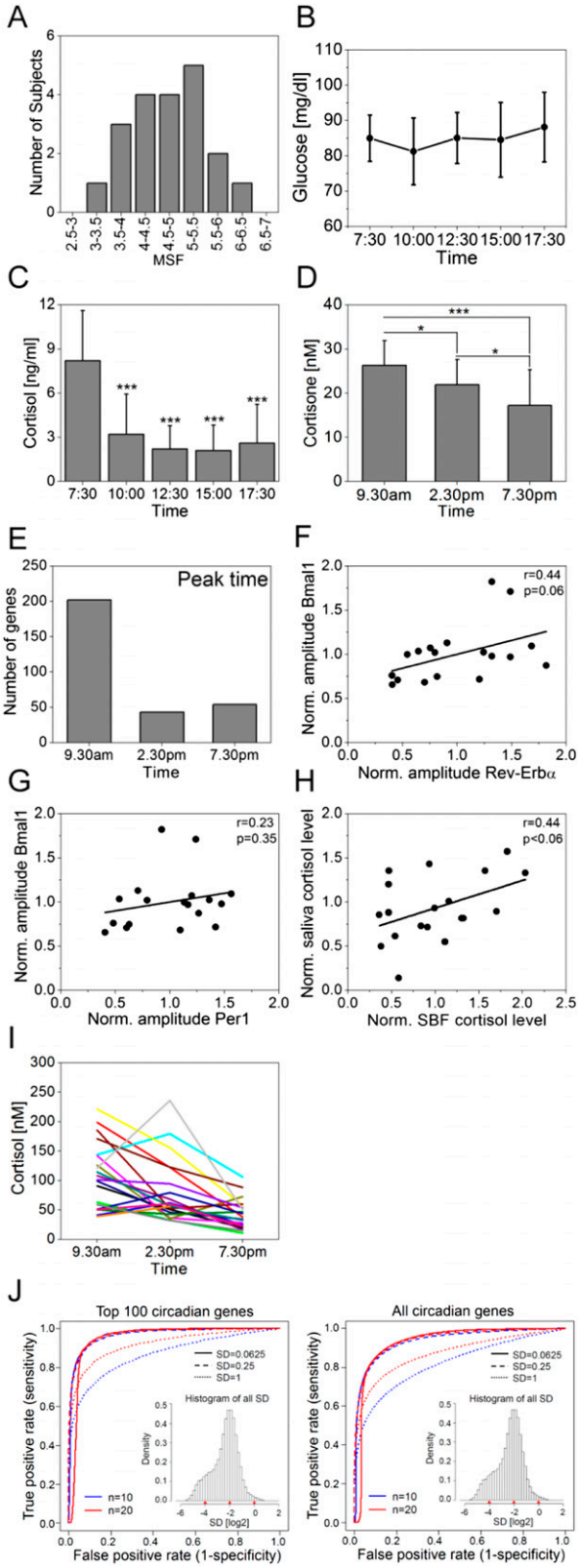

Fig. S1. Circadian control parameters in human subjects. (*A*) Chronotypes of individual subjects were determined using the MCTQ. Mid-sleep on free days (MSF) adjusted for individual average sleep need (1) of all 20 participants of the suction blister study is depicted. No subjects with extreme chronotypes participated in the study. (*B*) Because food intake is known to affect the circadian phase of peripheral oscillators (2), equicaloric meals were provided in regular intervals throughout the day, resulting in constant blood glucose levels during the study (n = 20 mean value ± SD). No significant variation in glucose levels was found in individual subjects or in mean values of 20 subjects. (*C* and *D*) Cortisol/cortisone levels of saliva (*C*) and suction-blister liquid (*D*) were determined at the indicated time (n = 20; mean value ± SD). *$P < 0.05$; ***$P < 0.001$ (Mann–Whitney U test; in *C*, *** indicates P value obtained from tests against morning

Legend continued on following page

cortisol levels). (*E*) Peak phase distribution of significantly ($q < 0.05$) regulated genes. (*F* and *G*) Normalized (relative to mean value of all subjects) amplitudes (maximum expression minus minimum expression) of depicted genes were correlated. A linear fit is depicted and Pearson's correlation coefficient (*r*) and the corresponding *P* value are shown. Amplitudes of *Bmal1* and *Rev-Erbα* show a weak correlation ($P = 0.06$), whereas *Bmal1* and *Per1* amplitudes show no correlation ($P = 0.35$). (*H*) Normalized (relative to mean value of all subjects) morning cortisol levels of saliva and suction-blister fluid were correlated. A linear fit is depicted and Pearson's correlation coefficient ($r = 0.44$) and the corresponding *P* value ($P < 0.06$) indicate a weak correlation. (*I*) Individual cortisol levels of all 20 subjects in suction-blister liquid obtained at indicated times are shown (compare Fig. 1*A*). (*J*) ROC curve for a simulated three-point sampling strategy in a 48-h time series (see *SI Materials and Methods, Simulation of Three Time-Point Sampling* for details). ROC curves were generated for semisynthetic gene sets with three different realistic SDs and sample sets corresponding to 10 or 20 individual subjects as indicated. *Insets* show SD distribution of our suction-blister microarray dataset as histogram. (*Left*) Recovery of the top 100 circadian genes. (*Right*) Recovery of all circadian genes. AUC values are between 0.82 and 0.97, indicating very good sensitivity and specificity (see *SI Materials and Methods, Simulation of Three Time-Point Sampling* for details).

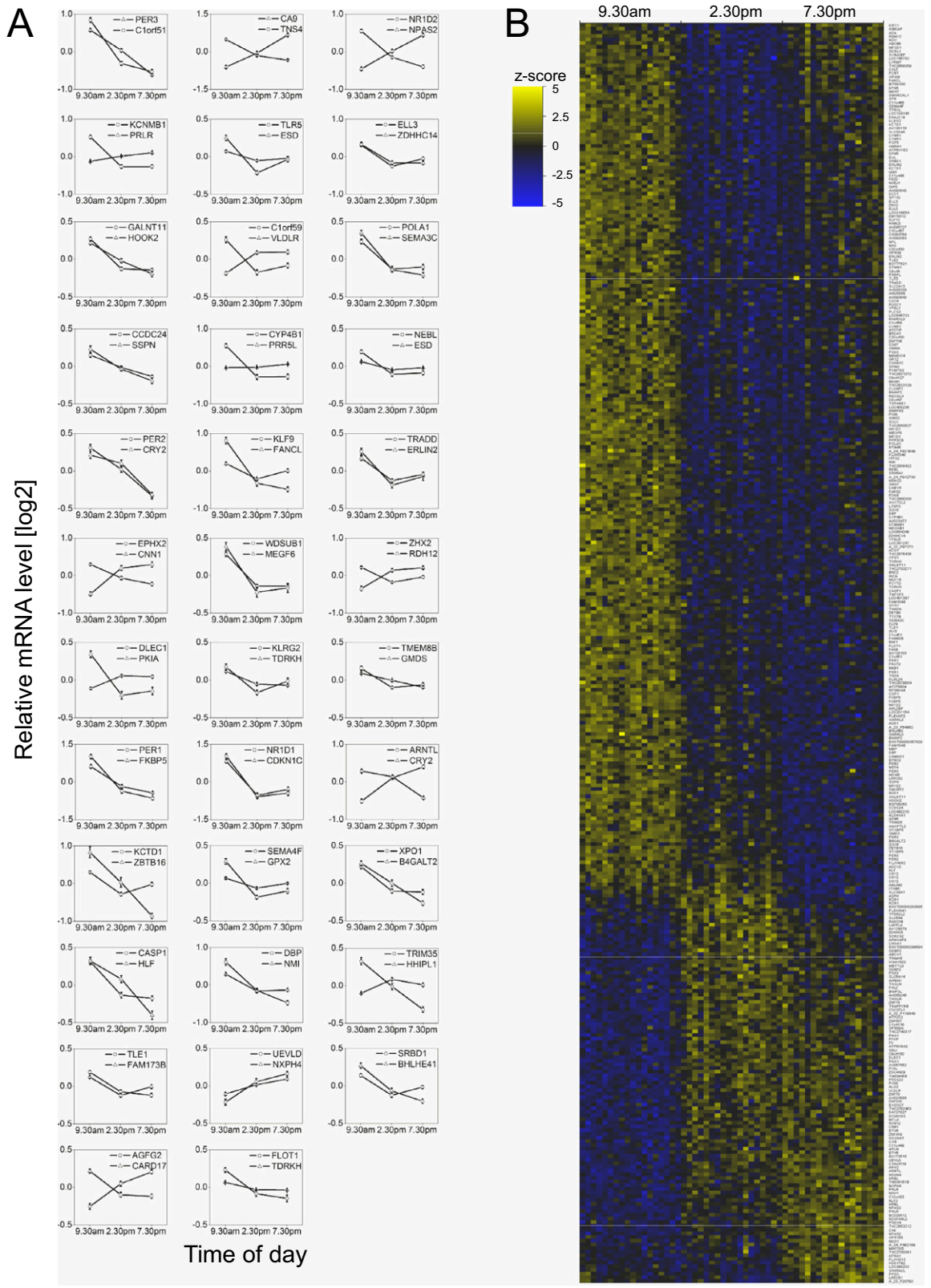

Fig. S2. Circadian transcriptome in human epidermis. (*A*) Log2 gene expression of the 70 most significant genes is depicted relative to mean expression. Error bars indicate SEM (n = 19 subjects). (*B*) Heat map of all significant probe sets. Microarray data were first centered for each subject by subtracting the mean from each value of the three time points to remove magnitude differences. Then, all data of a probe set were fitted to a sinus function to estimate the peak time, and z scores were calculated for each probe set over all subjects and time points. Data were plotted as a heat map using the image() function of "R" with a blue-yellow color code as indicated below the figure. Rows were ordered according to the peak time of the probe sets. Columns were grouped into three blocks according to the three time points, as indicated above the heat map. The order within each block is according to the ID no. of each subject. Gene symbols for each row are depicted at right.

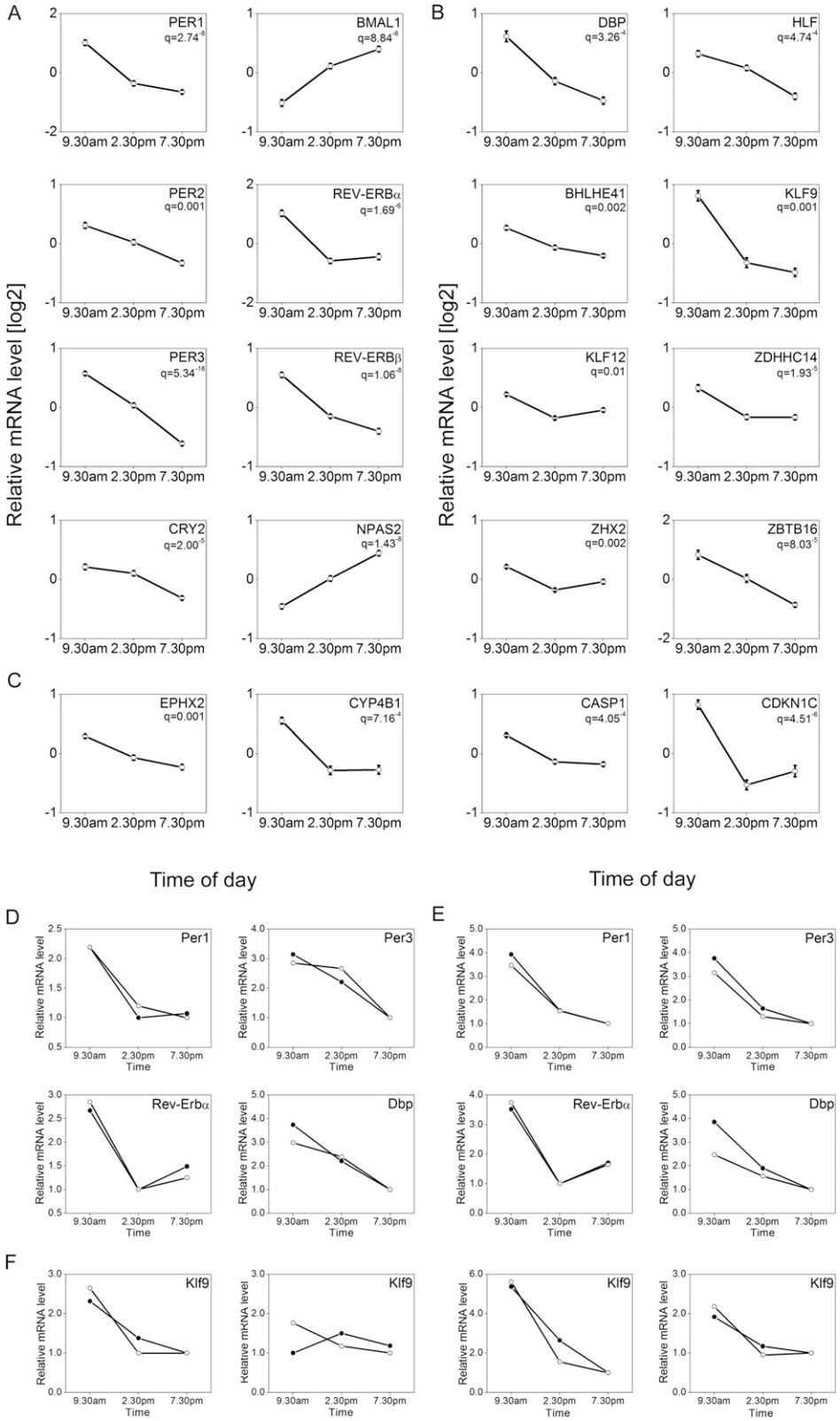

Fig. S3. Circadian gene expression of clock genes and selected output genes. Log2 gene expression levels of depicted genes are given as mean value of 19 subjects ± SEM. (*A*) Canonical clock genes. (*B*) Transcription factors. (*C*) Rate-limiting enzymes. Per1, $q = 2.74^{-8}$; Per2, $q = 0.001$; Per3, $q = 5.34^{-18}$; Cry2, $q = 2.00^{-5}$; Bmal1, $q = 8.84^{-6}$; Rev-Erbα, $q = 1.69^{-6}$; Rev-Erbβ, $q = 1.06^{-8}$; Npas2, $q = 1.43^{-8}$; Dbp, $q = 3.26^{-4}$; Bhlhe41, $q = 0.002$; Klf9, $q = 0.001$; Klf12, $q = 0.01$; Zdhhc14, $q = 1.93^{-5}$; Zhx2, $q = 0.002$; Hlf, $q = 4.74^{-4}$; Zbtb16, $q = 8.03^{-5}$; Ephx2, $q = 0.001$; Cyp4b1, $q = 7.16^{-4}$; Casp1, $q = 4.05^{-4}$; Cdkn1c, $q = 4.51^{-6}$. (*D–F*) qPCR validation. (*D* and *E*) Microarray measurements (open circles) of canonical clock genes from two individuals (*D* and *E*) were compared with qPCR measurements (filled circles) at the indicated time. (*F*) Microarray measurements (open circles) of Klf9 expression levels from four individuals were compared with qPCR measurements (filled circles) at the indicated time. For relative quantification, qPCR gene expression levels were normalized to nonoscillating 18S ribosomal RNA and are given relative to minimum expression.

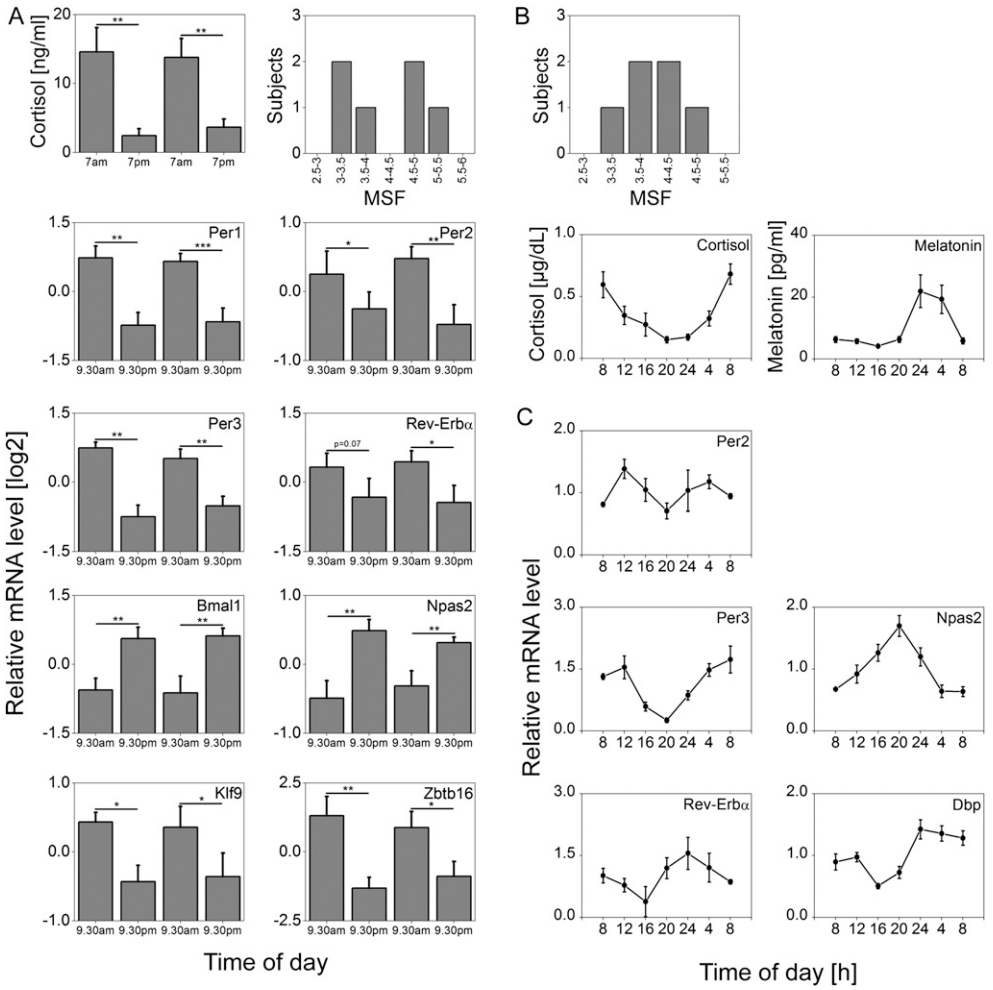

Fig. S4. Validation of circadian gene expression in human epidermis. (*A*) Cortisol levels were determined in saliva samples at the indicated times (mean of six subjects ± SEM). Mid-sleep on free days (MSF) adjusted for individual average sleep need is depicted for each subject (*Upper Right*). Gene expression of depicted genes in suction-blister epidermis obtained over 48 h at the indicated time are given as log2 expression levels (ΔCT values) of six subjects ± SEM relative to the 24-h mean. $*P < 0.05$; $**P < 0.01$; $***P < 0.001$ (*t* test). (*B*, *Top*) Mid-sleep on free days (MSF) adjusted for individual average sleep need is depicted for each subject. Cortisol and melatonin levels are given as mean of six subjects ± SEM. (*C*) Gene expression of depicted genes in the epidermis of punch biopsies obtained over 24 h at the indicated times are shown relative to the 24 h mean expression (six subjects ± SEM). Per3, Npas2, Dbp: $P < 0.001$; Nr1d1: $P = 0.006$; Per2 $P = 0.19$ (CircWave analysis).

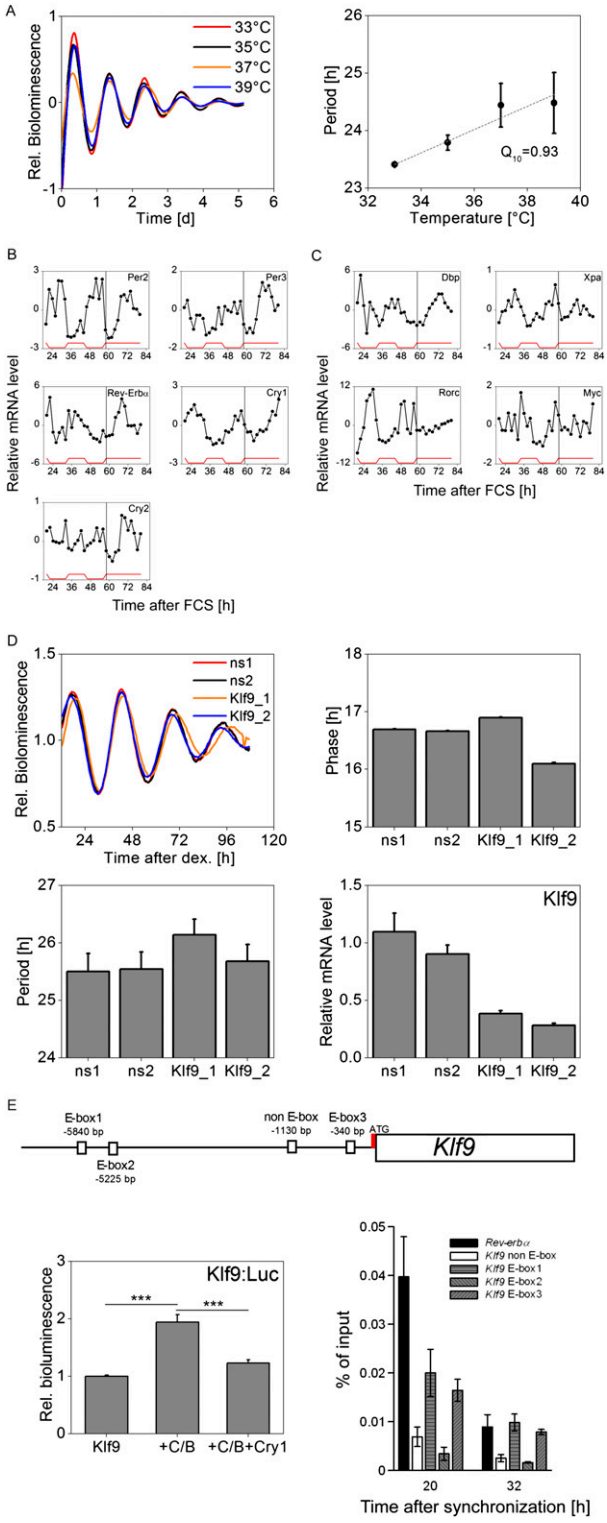

Fig. S5. Characteristics of the keratinocyte oscillator. (*A*) Temperature compensation of the keratinocyte oscillator. HaCaT cells carrying a *Bmal1:luc* promoter reporter (3) were synchronized with a single dex pulse and cultured at either 33, 35, 37, or 39 °C while monitoring bioluminescence over 5 d (*Left*). Circadian periods were determined as described previously (4). Error bars indicate minimum and maximum of two individual cultures. (*Right*) Linear fit is indicated by a dashed gray line. The calculated Q_{10} value is 0.93. (*B*) Primary keratinocytes were synchronized similar to Fig. 2*B*. Cells were harvested in regular 2-h intervals starting 24 h after FCS for 60 h, and mRNA levels of depicted genes were determined. Expression levels are given relative to mean expression. (*B*) Canonical clock genes. (*C*) Clock-controlled genes. Statistical analysis for circadian gene expression was performed using CircWave software. Per2, Per3, Cry1, Rev-Erbα, Xpa, Rorc: $P < 0.001$; Dbp: $P = 0.001$; Cry2: $P = 0.02$; Myc: $P = 0.15$. (*P* values of each tested gene during temperature entrainment and constant conditions are given in Table S1C.) (*D*) Bioluminescence recordings of U2OS *Bmal1:Luc* reporter cells carrying lentivirally delivered anti-*Klf9* (Klf9_1, Klf9_2) or nonsilencing (ns1, ns2) shRNAs were performed as described (4). Phases and periods are shown as mean values of six measurements ± SD. *Klf9* mRNA levels are shown relative to nonsilencing controls (mean value ± SD of four individual cultures). (*E*, *Upper*) *Klf9* gene is schematically depicted. Identified E-Boxes, as well as

Legend continued on following page

a non-E-Box control region and the ATG start codon, are indicated. (*Lower Left*) Cotransactivation assays using a 1,000-bp *Klf9*-fragment containing E-box3 fused to luciferase (*Klf9:luc*) were carried out in HEK293 cells. CLOCK/BMAL1-mediated twofold induction of *Klf9:luc* reporter is repressed by the cotransfection of CRY1. Error bars indicate SEM (n = 12 wells from four independent experiments). ***$P < 0.001$ (t test). (*Lower Right*) ChIP analysis of BMAL1 binding to regions containing the three E-boxes or to the non-E-box containing region of the *Klf9* gene; BMAL1 binding to the *Rev-erbα* gene served as positive control. ChIP was performed in human U2OS cells harvested at 20 and 32 h after synchronization. Averages of four measurements (± SD) are shown.

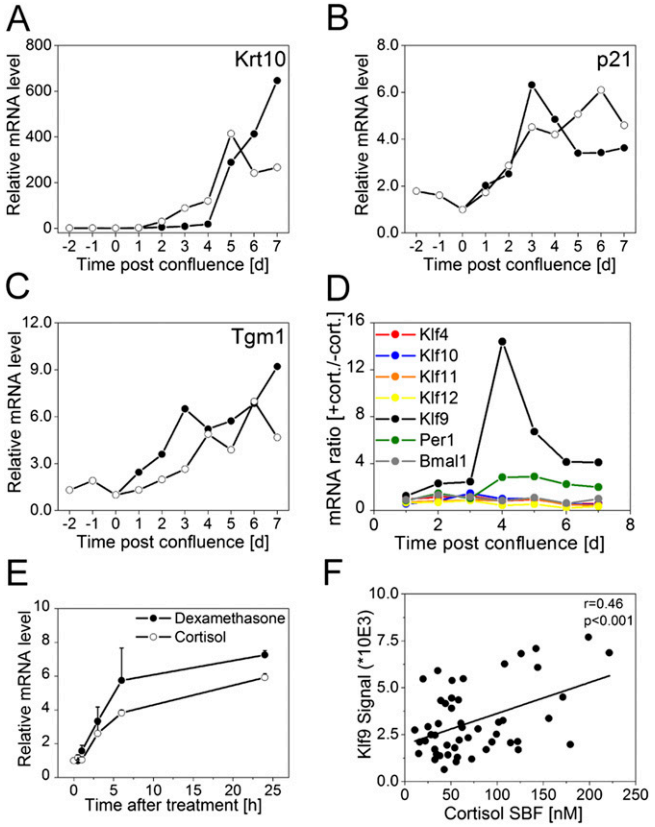

Fig. S6. Cortisol-dependent gene expression in primary keratinocytes. (*A*–*C*) Primary keratinocytes were cultivated in full KGM growth medium until reaching confluence. Subsequently, cells were either left in full KGM (filled circles) or transferred to autocrine media lacking growth factors (open circles) and harvested each day for 7 consecutive days. Expression levels of depicted genes were normalized to 18S ribosomal RNA and are given relative to minimum expression (representative result of repeated experiments). (*D*) Cells were treated similar to Fig. 3*C* and mRNA ratios [autocrine cultures (+cortisol)/autocrine cultures (−cortisol)] of depicted genes at the indicated time postconfluence are shown (representative result of repeated experiments). (*E*) Keratinocytes were treated with dex or cortisol and harvested 0.5, 1, 3, 7, and 24 h after treatment. *Klf9* mRNA levels of two experiments (mean ± maximum or minimum) are shown relative to cells treated with solvent only. (*F*) Cortisol levels obtained from suction-blister liquid of 20 individuals throughout the day were plotted against corresponding *Klf9* microarray signal intensities from suction-blister epidermis. A linear fit is depicted, and Pearson's correlation coefficient (r = 0.46) and the corresponding P value ($P < 0.001$) indicate a weak but significant correlation.

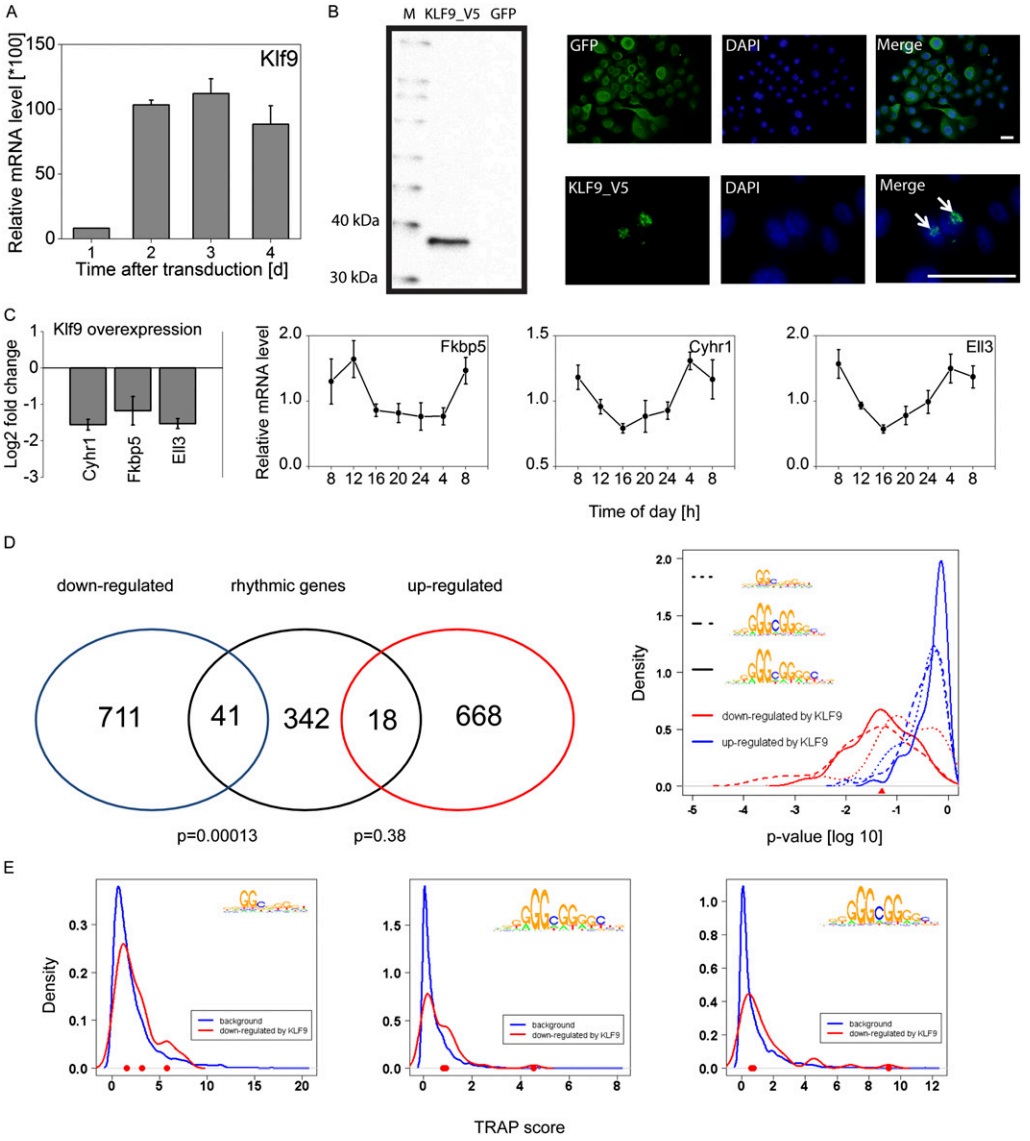

Fig. S7. *Klf9* overexpression in primary keratinocytes. The *Klf9* ORF was cloned into a lentiviral expression plasmid (pLenti6) and stably integrated into primary human keratinocytes. (*A*) *Klf9* overexpression levels in primary keratinocytes 1–4 d after transduction are shown relative to GFP control cells. (Selection medium containing blasticidin was applied for 1d 24 h after viral transduction; mean ± SD of two experiments.) (*B*) Expression of the KLF9_V5 fusion protein (expected size, 33 kDa) was confirmed using Western blot analysis (anti-V5 antibody) in KLF9_V5 but not GFP-expressing control cells. Cellular localization was studied using immunocytochemistry. KLF9_V5 and GFP control cells were fixed and labeled 2 d after infection using V5- or GFP-specific antibodies, respectively, and nuclei were counterstained using DAPI. White arrowheads indicate nuclear localization of the KLF9_V5 signal. (Cells were cultivated without selection agent; note that cells in the center are positive for KLF9_V5, whereas adjacent cells are negative, i.e., not transduced.) (Scale bar: 50 μm.) (*C*, *Left*) Log2 mRNA fold changes (FC) of putative *Klf9* target genes in KLF9-overexpressing primary keratinocytes obtained from microarray analysis. Mean FC ± SD of three expression values (measured 2, 4, and 7 d after transduction) are shown relative to GFP control cells. Gene expression of depicted genes in the epidermis of punch biopsies obtained over 24 h at the indicated times are shown relative to the 24-h mean expression (five subjects ± SEM). *Cyhr1*, *Ell3*: $P < 0.001$; *Fkbp5*: $P = 0.01$ (CircWave analysis). (*D*, *Left*) Venn diagram of genes that are expressed in a daytime-dependent manner in suction-blister epidermis (rhythmic genes) and genes regulated by KLF9 overexpression (down-regulated and up-regulated). *P* values indicate significance for over-representation (Fisher's test). (*Right*) *P* value distribution of TRAP scores for depicted *Klf9*-binding motifs are shown in a density plot for gene sets that are down- and up-regulated by KLF9 (red and blue curves, respectively) compared with many corresponding background gene sets (see *SI Material and Methods, Promoter analysis* for details). (*E*) TRAP-score density for depicted KLF9-binding motifs is shown for genes down-regulated by KLF9 and a corresponding background set. TRAP scores for *Cyhr1*, *Ell3*, and *Fkbp5* are indicated as red dots.

1. Roenneberg T, et al. (2004) A marker for the end of adolescence. *Curr Biol* 14:R1038–R1039.
2. Damiola F, et al. (2000) Restricted feeding uncouples circadian oscillators in peripheral tissues from the central pacemaker in the suprachiasmatic nucleus. *Genes Dev* 14:2950–2961.
3. Spörl F, et al. (2011) A circadian clock in HaCaT keratinocytes. *J Invest Dermatol* 131:338–348.
4. Maier B, et al. (2009) A large-scale functional RNAi screen reveals a role for CK2 in the mammalian circadian clock. *Genes Dev* 23:708–718.

Other Supporting Information Files

Table S1 (XLSX)
Table S2 (DOCX)